PHYSICAL REVIEW A VOLUME 58, NUMBER 1 JULY 1998

Nonlinear frequency conversion with short laser pulses and maximum atomic coherence

Lu Deng,[1,2] M. G. Payne,[1] and W. R. Garrett[3,4]
[1]*Department of Physics, Georgia Southern University, Statesboro, Georgia 30460-8031*
[2]*Atomic Physics Division, National Institute of Standards and Technology, Gaithersburg, Maryland 20899*
[3]*Oak Ridge National Laboratory, Oak Ridge, Tennessee 37831-2008*
[4]*Department of Physics, University of Tennessee, Knoxville, Tennessee 37996*
(Received 24 December 1997; revised manuscript received 10 February 1998)

A perturbation treatment for Raman generation with a combination of long, short, and delayed laser pulses is presented. When the coupling and probe lasers are applied in a counterintuitive sequence, the fast oscillatory contributions to populations and coherence are eliminated by robust adiabatic passage, allowing a much simpler solution to the problem. Such counterintuitive and on-resonance operation allows effective electromagnetically induced transparency to evolve so that the probe laser photons will experience no absorption yet still fully participate in the nonlinear frequency conversion. Consequently, better conversion efficiency should be possible. [S1050-2947(98)08607-7]

PACS number(s): 42.65.Ky

INTRODUCTION

Electromagnetically induced transparency (EIT) [1–3] describes the phenomena whereby a medium that is normally opaque to a probe laser tuned to a resonant transition can be made transparent when a coupling laser is also applied simultaneously. In a resonant three-level system, such a process drives the atoms to a population trapped state, and has been observed both in continuous-wave and pulsed operations. When both lasers are pulsed, the EIT processes are particularly interesting, and conditions (such as pulse shape, timing, adiabaticity, etc.) for which the transparency is established have been widely studied [1–5]. Recently, it has been shown [6] that EIT can also be used to prepare an atomic system for more efficient frequency conversion. This is not surprising, since the EIT process involves adiabatic coherent population transfer, a process that is dependent upon the pulse shapes and delay. Careful manipulation of the pulse shapes and sequence would allow one to control the adiabatic passage process and optimize the nonlinear conversion efficiency. An added advantage is the elimination of the probe absorption, which limits the effective interaction length. In this communication we extend this concept to the short pulse regime and examine the validity of the approximations used in the previous study. Specifically, we seek to avoid approximations adopted in a previous treatment of Raman generation [6], which are not always appropriate. We show that when the width of the source pulse is not much less than that of the coupling and probe pulses, the Raman coherence changes appreciably during the time when the source pulse is present, hence the previous assumption [6] that $|\rho_{10}|\simeq 0.5$ is not always appropriate. Second, we show that even in the case of a nondepleted source pulse, populations of the states must be included in the Maxwell equation, and the maximum Raman coherence does *not* always lead to the maximum conversion efficiency. Moreover, we show that when the source depletion cannot be neglected, as is usually the case for efficient frequency conversion process, the populations of the two lower states must be kept and the Maxwell equations for both the generated field and the depleted source field must be solved simultaneously with *populations* and *Raman coherence*. Based on the following adiabatic approximation with delayed pulses, we point out that these conditions are much more satisfactory when the source pulse is much shorter than the coupling and probe laser pulses.

THE MODEL AND THE EQUATIONS OF MOTION

Our objective is to examine conditions for efficient stimulated Raman generation with short pulses and the dependency of such a frequency conversion process on the atomic coherence. Consider a three-state system in which a very intense coupling laser is tuned onto the $|1\rangle\rightarrow|2\rangle$ transition (see Fig. 1). We assume that all lasers are unfocused and the plane-wave approximation is applicable. When a probe laser is tuned to the line center of the $|0\rangle\rightarrow|2\rangle$ transition, it is easily seen that the probe laser experiences no absorption due to the fact that the contributions to the index from the members of the induced Autler-Townes doublet cancel each other. We assume that these two lasers are of the same pulse profile (Fig. 2) and have the same pulse duration of a few ns.

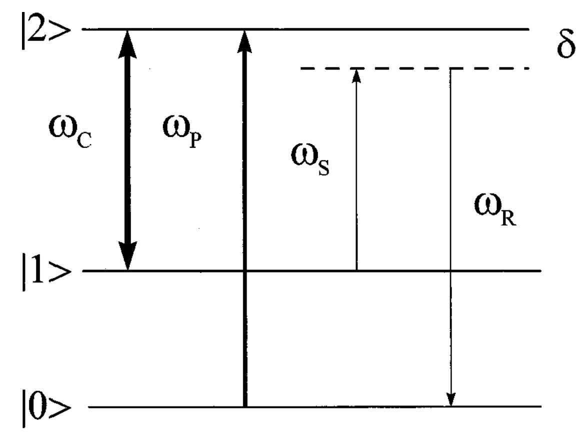

FIG. 1. Energy-level diagram showing relevant laser coupling schemes. ω_c, ω_p, ω_S, and ω_R are frequencies of coupling, probe, source, and Raman field, respectively.

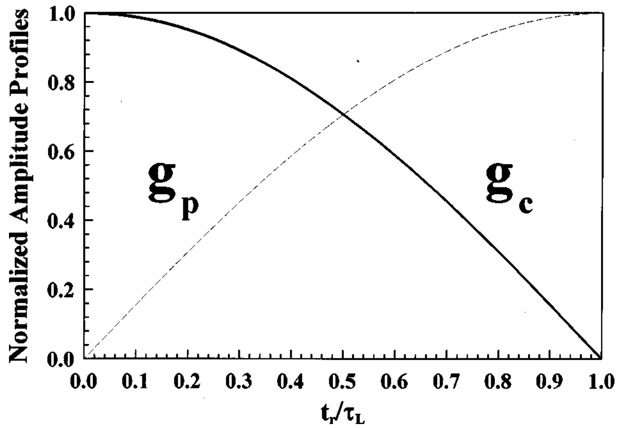

FIG. 2. Coupling and probe laser field amplitude profiles as functions of t_r/τ_L.

We now introduce a short pulse (a few ps) that couples the states $|1\rangle$ and $|2\rangle$ with a detuning of about $1000\ \mathrm{cm}^{-1}$. This laser is usually weak, and we are interested in the Raman generation from state $|2\rangle$ to $|0\rangle$. The situation presented here is similar to the recent experimental arrangement described in Ref. [6], except that the pulse duration for the source laser is much shorter than for the coupling and probe lasers, and the delay between the long pulsed lasers may be as long as a few ns.

We first write the wave function of the system as

$$|\Psi(t)\rangle=\sum_{n=0}^{2} A_n(t)e^{-i\omega_n t}|n\rangle, \tag{1}$$

where A_n is a slowly varying quantity. We now substitute this wave function into the Schrödinger equation

$$i\hbar\frac{\partial|\Psi(t)\rangle}{\partial t}=\hat{H}|\Psi(t)\rangle=(\hat{H}_0-\hat{\vec{D}}\cdot\hat{\vec{E}})|\Psi(t)\rangle, \tag{2}$$

where

$$\vec{E}=\frac{1}{2}\sum_{\alpha}\vec{E}_\alpha^{(+)}(t)e^{ik_\alpha z-i\omega_\alpha t}+\text{c.c.}, \tag{3}$$

where $\alpha=c$ (coupling), p (probe), S (source), and R (Raman). Equation (2) gives three coupled first-order differential equations:

$$\begin{aligned}
\frac{\partial A_0}{\partial t_r}&=i[\Omega_{02}^{(p)}e^{-ik_pz}+\Omega_{02}^{(R)}e^{-ik_Rz-i\delta(t_r+z/c)}]A_2,\\
\frac{\partial A_1}{\partial t_r}&=i[\Omega_{12}^{(c)}e^{-ik_cz}+\Omega_{12}^{(S)}e^{-ik_Sz-i\delta(t_r+z/c)}]A_2,\\
\frac{\partial A_2}{\partial t_r}&=i[\Omega_{20}^{(p)}e^{ik_pz}+\Omega_{20}^{(R)}e^{ik_Rz+i\delta(t_r+z/c)}]A_0\\
&\quad+i[\Omega_{21}^{(c)}e^{ik_cz}+\Omega_{21}^{(S)}e^{ik_Sz+i\delta(t_r+z/c)}]A_1,
\end{aligned} \tag{4}$$

where we have expressed time-dependent quantities in terms of the retarded time $t_r=t-z/c$ which will be used later in solving Maxwell's equations. We assume that initially the atom is in the ground state $|0\rangle$ and the coupling and probe lasers are applied in a counterintuitive sequence. That is, the coupling laser (for $|1\rangle\rightarrow|2\rangle$ transition) is applied first, and the probe laser (for $|0\rangle\rightarrow|2\rangle$ transition) is applied at a delayed time. We will show that such a procedure eliminates the difficulty in the adiabatic-following treatment normally encountered at an early stage of the pulse when the lasers are tuned on resonance, hence enabling a reliable adiabatic solution to the problem in hand. Mathematically, we choose

$$\begin{gathered}
\Omega_{02}^{(p)}=\Omega_p(0)g_p(t-z/c)=\Omega g_p(t_r),\\
\Omega_{12}^{(c)}=\Omega_c(0)g_c(t-z/c)=\Omega g_c(t_r),\\
\Omega_{02}^{(R)}=\Omega_R(t_r),\\
\Omega_{12}^{(S)}=\Omega_S(t-z/c)=\Omega_S g_S(t_r),\\
g_p=g_p(t_r)=\sin\left(\frac{\pi t_r}{2\tau_L}\right),\\
g_c=g_c(t_r)=\cos\left(\frac{\pi t_r}{2\tau_L}\right),\\
g_S=g_S(t_r)=e^{-(t_r-t_{r0})^2/\tau_S^2}.
\end{gathered} \tag{5}$$

In Eq. (5), we have used $\Omega_p(0)=\Omega_c(0)=\Omega$ for mathematical simplicity. We have also assumed that the half width of the long pulse is τ_L, while the half width of the short pulse with Gaussian profile is given by $\tau_S\sqrt{\ln 2}$. In a typical experiment, $\tau_L\simeq 10-40$ ns, and $\tau_S\sqrt{\ln 2}\simeq 1-10$ps so that $\tau_L\gg\tau_S\sqrt{\ln 2}$. The delay time for the short pulse is denoted by t_{r0}, and we have chosen a fixed delay of $t_{r0}/\tau_L\simeq 0.5$. Later, we will see that the choice of delay depends on the system at hand. Using Eq. (5), we can rewrite Eq. (4) as

$$\begin{aligned}
\frac{\partial A_0}{\partial t_r}&=i[\Omega g_pe^{-ik_pz}+\Omega_R(t_r)e^{-ik_Rz-i\delta(t_r+z/c)}]A_2,\\
\frac{\partial A_1}{\partial t_r}&=i[\Omega g_ce^{-ik_cz}+\Omega_S(t_r)e^{-ik_Sz-i\delta(t_r+z/c)}]A_2,\\
\frac{\partial A_2}{\partial t_r}&=i[\Omega^*g_pe^{ik_pz}+\Omega_R^*(t_r)e^{ik_Rz+i\delta(t_r+z/c)}]A_0\\
&\quad+i[\Omega^*g_ce^{ik_cz}+\Omega_S^*(t_r)e^{ik_Sz+i\delta(t_r+z/c)}]A_1.
\end{aligned} \tag{6}$$

In the above equations, we have suppressed the z parameter in both Ω_R and Ω_S. Our perturbation scheme proceeds with the following steps. First, in Eq. (6) we neglect terms containing Ω_S and Ω_R, since the first two long-pulse lasers are assumed to be very intense [in a typical operation, $\Omega_c(0)=\Omega_p(0)\simeq$ several cm^{-1}]. The solution of the simplified equations is then used to solve Eq. (6) to first order in Ω_S or Ω_R. Finally, the wave function is used to construct the nonlinear polarization, which in turn will be used as the source term in Maxwell's equation for the generated field. Such a small signal-gain method will permit a tractable solution to the problem and offer some insight into how to further reduce the complexity of the problem.

SOLUTIONS AND DISCUSSIONS

Following the above-described procedure, we first solve

$$\frac{\partial A_0^{(0)}}{\partial t}=i\Omega g_p(t_r)e^{-ik_pz}A_2^{(0)},$$

$$\frac{\partial A_1^{(0)}}{\partial t}=i\Omega g_c(t_r)e^{-ik_cz}A_2^{(0)}, \tag{7}$$

$$\frac{\partial A_2^{(0)}}{\partial t}=i\Omega^* g_p(t_r)e^{ik_pz}A_0^{(0)}+i\Omega^* g_c(t_r)e^{ik_cz}A_1^{(0)}.$$

This set of first-order differential equations with several pulse profiles including Eq. (5) and different adiabatic treatments have been widely studied [7]. The solutions to Eq. (7) are

$$A_0^{(0)}=1-\frac{|\Omega|^2\tau_L^2\pi}{2\beta^2}\left(\frac{\cos(\alpha+\beta)\eta-1}{2(\alpha+\beta)}+\frac{\cos(\alpha-\beta)\eta-1}{2(\alpha-\beta)}-\frac{\cos\,\alpha\eta-1}{\alpha}\right),$$

$$A_1^{(0)}=\frac{|\Omega|^2\tau_L^2\pi}{2\beta^2}\,e^{i(k_p-k_c)z}\left(\frac{\sin(\alpha+\beta)\eta}{2(\alpha+\beta)}+\frac{\sin(\alpha-\beta)\eta}{2(\alpha-\beta)}-\frac{\sin\,\alpha\eta}{\alpha}\right), \tag{8}$$

$$A_2^{(0)}=-i\,\frac{\Omega^*\tau_L\pi}{2\beta^2}\,e^{ik_pz}(\cos\,\beta\eta-1),$$

where

$$\alpha=\frac{\pi}{2},\quad \beta=\sqrt{\frac{\pi^2}{4}+|\Omega|^2\tau_L^2},\quad \eta=\frac{t_r}{\tau_L}.$$

When $|\Omega|\tau_L \gg 1$, these amplitudes are simplified to

$$A_0^{(0)}\simeq\cos\,\alpha\eta,\;\; A_1^{(0)}\simeq -e^{i(k_p-k_c)z}\sin\,\alpha\eta,\;\; A_2^{(0)}\simeq 0, \tag{9}$$

i.e., the rapid oscillatory terms become much less important because of the adiabatic following. In Fig. 3 we have plotted populations ρ_{00}, ρ_{11}, ρ_{22} and coherence ρ_{10} constructed from Eq. (8) for $|\Omega|\tau_L\simeq 1000$. It is also seen that both populations and coherences evolve slowly on the time scale of the long pulse, as expected from the adiabatic following theory. Next, we let

$$A_n=A_n^{(0)}+A_n^{(1)},\;\;(n=0,1,2). \tag{10}$$

Substituting Eq. (10) into Eq. (6) and using Eq. (7), we obtain

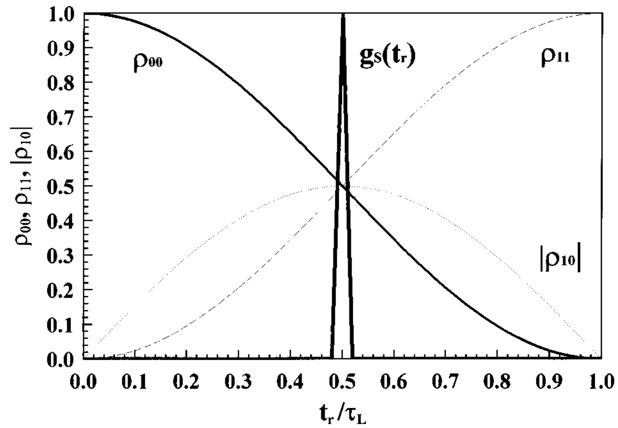

FIG. 3. Zeroth-order density-matrix elements as functions of t_r/τ_L, where τ_L is the pulse width of the coupling and probe lasers. In the center, a short pulse of Gaussian profile (not to scale) is also plotted for comparison of the time scale. Parameters used: $\Omega_p=\Omega_c=10\pi$ cm^{-1}, $\tau_L\simeq 10$ ns, $\tau_S\simeq 10$ ps, and $\rho_{22}\simeq 0$.

$$\frac{\partial A_0^{(1)}}{\partial t_r}=i[\Omega g_pe^{-ik_pz}A_2^{(1)}+\Omega_R(t_r)e^{-ik_Rz-i\delta(t_r+z/c)}A_2^{(0)}],$$

$$\frac{\partial A_1^{(1)}}{\partial t_r}=i[\Omega g_ce^{-ik_cz}A_2^{(1)}+\Omega_S(t_r)e^{-ik_Sz-i\delta(t_r+z/c)}A_2^{(0)}], \tag{11}$$

$$\frac{\partial A_2^{(1)}}{\partial t_r}=i[\Omega^* g_pe^{ik_pz}A_0^{(1)}+\Omega^* g_ce^{ik_cz}A_1^{(1)}]+i[\Omega_R^*(t_r)e^{ik_Rz}A_0^{(0)}+\Omega_S^*(t_r)e^{ik_Sz}A_1^{(0)}]e^{i\delta(t_r+z/c)}.$$

Since $\delta\tau_L$, $\delta\tau_S \gg 1$, and $A_2^{(0)}\ll 1$, we have the following set of adiabatic solutions:

$$A_0^{(1)}\simeq-\frac{\Omega_R(t_r)e^{-ik_Rz-i\delta(t_r+z/c)}}{\delta}A_2^{(0)},$$

$$A_1^{(1)}\simeq-\frac{\Omega_S(t_r)e^{-ik_Sz-i\delta(t_r+z/c)}}{\delta}A_2^{(0)}, \tag{12}$$

$$A_2^{(1)}\simeq\frac{\Omega_R^*(t_r)e^{ik_Rz+i\delta(t_r+z/c)}}{\delta}A_0^{(0)}+\frac{\Omega_S^*(t_r)e^{ik_Sz+i\delta(t_r+z/c)}}{\delta}A_1^{(0)}.$$

We now calculate the polarization $P=N\langle\Psi|\hat{D}|\Psi\rangle$, where

$$|\Psi\rangle=\sum_{n=0}^{2}(A_n^{(0)}+A_n^{(1)})e^{-i\omega_nt}|n\rangle. \tag{13}$$

The Raman polarization of positive frequency is given by

$$P^{(+)}(\omega_R)\simeq ND_{02}(A_0^{(0)*}A_2^{(1)}+A_0^{(1)*}A_2^{(0)})e^{i\omega_{20}t}$$
$$\simeq \frac{ND_{02}}{\delta}\, e^{-i\omega_R t_r}[\Omega_R^*(t_r)|A_0^{(0)}|^2 + \Omega_S^*(t_r)e^{i(k_S-k_R)z}A_0^{(0)*}A_1^{(0)}]. \tag{14}$$

Maxwell's equation for the generated field in the retarded frame is given by

$$\left(\frac{\partial\Omega_R^*}{\partial z}\right)_{t_r} e^{-i\omega_R t_r} = -\frac{2i\pi D_{20}}{\hbar c\omega_R}\frac{\partial^2 P^{(+)}(\omega_R)}{\partial {t_r}^2}, \tag{15}$$

where we have let $\Omega_R^* = D_{20}E_R^{(+)}/2\hbar$. Using Eq. (14) we obtain

$$\left(\frac{\partial\Omega_R^*}{\partial z}\right)_{t_r} \simeq i\,\frac{\kappa_{20}}{\delta}\,[\Omega_R^*(t_r)\rho_{00}+e^{i\Delta kz}\Omega_S^*(t_r)\rho_{10}]. \tag{16}$$

Similarly, for the source field we have

$$\left(\frac{\partial\Omega_S^*}{\partial z}\right)_{t_r} \simeq i\,\frac{\kappa_{21}}{\delta}\,[e^{-i\Delta kz}\Omega_R^*(t_r)\rho_{01}+\Omega_S^*(t_r)\rho_{11}], \tag{17}$$

where $\Omega_S^* = D_{21}E_S^{(+)}/2\hbar$. We have also introduced

$$\Delta k = k_p-k_c+k_S-k_R, \quad \kappa_{ij}=\frac{2\pi|D_{ij}|^2\omega_{ij}}{\hbar c},$$
$$\rho_{00}=|A_0^{(0)}|^2, \quad \rho_{11}=|A_1^{(0)}|^2, \quad \rho_{22}=|A_2^{(0)}|^2\ll 1, \tag{18}$$
$$\rho_{10}=e^{-i(k_p-k_c)z}A_0^{(0)*}A_1^{(0)}.$$

In deriving Eqs. (16) and (17) we have taken the factor $e^{i(k_p-k_c)z}$ out of density matrix elements in order to make the phase mismatch factor $e^{i\Delta kz}$ as seen. We have also neglected ρ_{22}, since it is always small in the present treatment. It is seen in Eqs. (16) and (17) that two types of contributions are involved in the generation of the Raman field. One is dependent upon the population differences between states $|0\rangle$, $|1\rangle$, and $|2\rangle$, and the other is dependent upon the Raman coherence ρ_{10}. In general, both contributions should be kept in order to treat the problem properly. The time-dependent terms in the populations and coherences will give rise to the usual ac-Stark-shifted resonance in the Raman spectrum. The result of including these time-dependent terms is a pair of difference equations in the frequency domain that are difficult to solve. However, an approximation that is valid in the case where the source pulse is much shorter than that of the coupling and probe pulses, as assumed in the present study, would allow a great simplification of Eqs. (16) and (17) while still preserving the essential physics of the problem. This approximation is quite evident in Fig. 3. We see that in the center of the time domain where the Raman coherence has reached its absolute maximum, both populations ρ_{00}, ρ_{11} and Raman coherence ρ_{10} are nearly constant during the time when the short source pulse is present. It is then reasonable to replace these quantities in Eqs. (16) and (17) with their local values at the center of the time domain so that in the frequency domain we will have two coupled first-order differential equations for the Raman spectrum that are readily solvable. It should, however, be pointed out that such an approximation is not appropriate if the pulse length of the source pulse is not very short in comparison with the coupling and probe pulses. For such a long source pulse the change of the populations and coherence will affect the generated field.

Case 1: The source (short) laser depletion is negligible

If the depletion of the source laser can be neglected, Ω_S may be treated as z independent, and we only need to deal with Eq. (16), which is immediately solvable. We obtain

$$\Omega_R^*(z,t_r)=i\,\frac{\kappa_{20}}{\delta}\,\Omega_S^*(0,t_r)\rho_{10}e^{i(\kappa_{20}/\delta)\rho_{00}z} \times\frac{e^{i[\Delta k-(\kappa_{20}/\delta)\rho_{00}]z}-1}{\Delta k-(\kappa_{20}/\delta)\rho_{00}}. \tag{19}$$

This result suggests that for phase-matched ($\Delta k=0$) nondepleted source operation, better conversion efficiency may be achieved by manipulating both Raman coherence ρ_{10} and population ρ_{00} while keeping $(\kappa_{20}\rho_{00})/\delta$ small. (Notice that the maximum efficiency *cannot* be achieved at the end of the coupling pulse where both ρ_{00} and $\rho_{10}\to 0$.) In the case of slight phase mismatch, the improved Raman conversion is also possible when $\Delta k=(\kappa_{20}\rho_{00})/\delta$, with $(\kappa_{20}\rho_{00})/\delta$ being kept small. In reality, when the conversion efficiency reaches a certain level, the depletion of the source pulse is inevitable. Thus, one must include the second Maxwell equation for the source field. As we will show below, this will lead to different conditions for which the conversion efficiency may be optimized.

Equation (19) also indicates that the generated field has a time profile similar to that of the source pulse (including the delay for the source pulse). This is because during the time when the short pulse is present, none of the atomic parameters change appreciably. Numerical simulation indicates that when the time-dependent terms in the density matrix elements are included, the frequency spectrum of the generated field will have sidebands corresponding to the ac Stark shifts due to the intense coupling and probe lasers. Another feature that distinguishes the present configuration from the usual Raman generation is that Eq. (16) does not support exponential gain as the usual Raman generation does. This may be explained in the following way. First, the coupling laser is very intense and the Rabi frequency would be very large so that spontaneous decay out of the state $|2\rangle$ has been neglected. Second, the EIT ensures that the probe laser experiences negligible or no absorption. Since the bandwidth and dephasing effects are neglected, detuning δ is real (otherwise an imaginary part would appear in δ). If these effects are included, terms that are proportional to these dephasing rates and laser bandwidths will appear on the right-hand side of Eq. (6) and result in a complex detuning appearing in the exponential factor on the right-hand side of Eq. (19). Consequently, an exponential Raman gain process could become dominant in the early stage [8,9].

Case 2: The source laser depletion is not negligible

Recent studies [6] of nonlinear frequency conversion in the nanosecond regime have shown that significant improvement of the conversion efficiency may be achieved by maximizing the Raman coherence at the preparation stage of the process (i.e., before the source pulse). Such high conversion efficiencies inevitably deplete the source beam. Hence, both Eqs. (16) and (17) must be solved simultaneously in order to correctly predict the generated Raman field.

Since we are mostly interested in the propagation effect, we will assume again that the time profile of the short pulse is described by Eq. (5). From Eqs. (16) and (17) we have

$$\frac{\partial \Omega_R^*}{\partial z} - iP_1\Omega_R^* = iQ_1\Omega_S^* e^{i\Delta kz}, \tag{20}$$

$$\frac{\partial \Omega_S^*}{\partial z} - iP_2\Omega_S^* = iQ_2\Omega_R^* e^{i\Delta kz}, \tag{21}$$

where

$$P_1 = \frac{\kappa_{20}}{\delta}\,\rho_{00}, \quad P_2 = \frac{\kappa_{21}}{\delta}\,\rho_{11}, \quad Q_1 = \frac{\kappa_{20}}{\delta}\,\rho_{10},$$

$$Q_2 = \frac{\kappa_{21}}{\delta}\,\rho_{01}.$$

With boundary conditions

$$\Omega_R^*(z=0,t_r) = 0, \quad \left.\frac{\partial \Omega_R^*}{\partial z}\right|_{z=0} = iQ_1\Omega_S^*(0,t_r), \tag{22}$$

Eqs. (20) and (21) can be solved immediately and yield

$$\Omega_R^*(z,t_r) = \frac{\kappa_{20}\Omega_S^*(0,t_r)\rho_{10}e^{i[(P_1+P_2+\Delta k)z/2]}}{2\,\delta S}\,(e^{iSz} - e^{-iSz}), \tag{23}$$

where

$$S = \frac{1}{2}\,\sqrt{(P_1+P_2+\Delta k)^2 + 4(Q_1Q_2 - P_1P_2 - P_1\Delta k)}. \tag{24}$$

Except for the population-dependent terms, Eq. (23) is identical to that given in Ref. [6]. We emphasize the importance of the population-dependent term since it is the interplay between populations and Raman coherence that dictates the optimized conversion efficiency. We again conclude from Eq. (23) that the Raman field does not have an exponential gain regime in the present treatment, as discussed above (here, S is always real). Nonetheless, it still supports high-efficiency nonlinear wave production. The conversion efficiency is given by

$$\eta = \frac{|\Omega_R^*|^2}{|\Omega_S^*|^2} = \frac{\kappa_{20}^2|\rho_{10}|^2}{\delta^2 S^2}\,\sin^2(Sz). \tag{25}$$

The maximum efficiency is obtained as

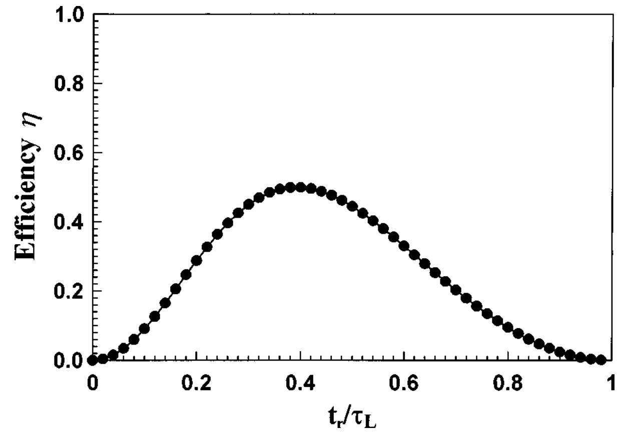

FIG. 4. Conversion efficiency as a function of t_r/τ_L. The optimized conversion efficiency for the system studied here is achieved near $t_r/\tau_L = 0.4$ instead of 0.5, where the absolute maximum Raman coherence is achieved.

$$\eta_{\max} = \frac{4|\rho_{10}|^2}{[\rho_{00} - (\kappa_{21}/\kappa_{20})\rho_{11}]^2 + 4(\kappa_{21}/\kappa_{20})|\rho_{10}|^2}. \tag{26}$$

Equation (26) predicts that the maximum conversion efficiency for the system studied here is achieved when the first term in the denominator becomes zero, which does *not* happen at the maximum ρ_{10}, as pointed out earlier (see also Fig. 3). However, if we take $\rho_{00} \simeq 1/2$, $\rho_{11} \simeq 1/2$, $|\rho_{10}| \simeq \frac{1}{2}$, and $\kappa_{21}/\kappa_{20} = 2$ we obtain $\eta \cong 0.43$. Experimentally, conversion efficiency as high as 0.4 has been obtained [6]. The higher conversion efficiency obtained in the present calculation can be attributed to the fact that dephasing and laser bandwidth were not included. In Fig. 4 we show the conversion efficiency of the present system at different delay times. One interesting feature is immediately obvious: the maximum conversion efficiency is *not* always achieved at the maximum Raman coherence. For the present system it is achieved shortly before the Raman coherence has reached its absolute maximum because of the contributions from population transferred. It is therefore preferable that one choose a suitable delay time for injecting the source pulse in order to optimize the conversion efficiency.

It should be pointed out that in the present treatment, we have assumed that the intensity distributions of the coupling and probe fields are of a sine-square shape, for mathematical simplicity. A Gaussian intensity distribution, which is wisely used in actual experiments, does *not* permit a clean treatment of the problem in hand, even for a zeroth-order perturbation solution. Physically, we do not expect to see a qualitative difference in the final result, due to the fact that the source pulse is much shorter, and the Raman field should have a profile similar to that of the source pulse regardless of the intensity profile of the coupling and probe fields. This can also be seen from Eq. (26) in the case of depleted source pulse. Using

$$1 = \rho_{00} + \rho_{11} + \rho_{22}, \qquad \rho_{22} \simeq 0, \tag{27}$$

we can recast Eq. (26) into

$$\eta_{\max}=\frac{1}{(\{\rho_{00}[1+(\kappa_{21}/\kappa_{20})]-(\kappa_{21}/\kappa_{20})\}^2/4|\rho_{10}|^2)+\kappa_{21}/\kappa_{20}}. \tag{28}$$

As long as similar adiabatic following conditions are met, different field profiles should not modify the density matrix elements dramatically and the conclusion should qualitatively stay the same [7]. The exact behavior of a realistic field profile may be obtained by numerically solving Eq. (6), since there is no analytical solution. In the case of different coupling and probe Rabi frequencies, no easy conclusion can be drawn without extensive numerics. If $|\Omega_c|\gg|\Omega_p|$ and the probe saturation is negligible, however, a quick observation can be made from Eq. (19). Under this circumstance, the ground-state population is nearly unchanged and the Raman coherence should be small, leading to a low conversion efficiency.

SUMMARY

In summary, we have examined the Raman generation with short-pulse and near-maximum atomic coherence. It is found that (1) adiabatic passage is very effective and atomic parameters evolve slowly on the scale of the long pulse so that during the time when the short pulse is present the density-matrix elements may be treated as constants (such an approximation is not quite appropriate for the case where all lasers have a similar pulse length); (2) very strong coupling and electromagnetically induced transparency (within the framework of the present treatment) have led to no exponential gain of the generated field, yet higher conversion efficiency is still possible; (3) the maximum Raman coherence does *not* always lead to the maximum efficiency and the optimized efficiency can be achieved by tailoring the timing of the delay of the source pulse.

ACKNOWLEDGMENTS

This research was partly sponsored by the National Science Foundation through Grant No. PHY-9540854, by NIST/Harvard University, and by the Georgia Southern Foundation. Helpful discussions with Dr. P. Lett, Dr. J. Lawall, and Dr. E. Hagley, all at NIST, are acknowledged. L. Deng would like to thank NIST/Harvard University for financial support, Dr. W. D. Phillips for hospitality and support, and Professor S. E. Harris for a reprint which stimulated the present study.

[1] K. J. Boller, A. Imamoglu, and S. E. Harris, Phys. Rev. Lett. **66**, 2593 (1991); O. A. Kocharovskaya and Y. I. Kahanin, Pis'ma Zh. Eksp. Teor. Fiz. **48**, 581 (1988) [JETP Lett. **48**, 630 (1988)]; M. Xiao, Y. Q. Li, S. Z. Jin, and J. Gea-Banacloche, Phys. Rev. Lett. **74**, 666 (1995); G. Z. Zhang, K. Hakuta, and B. P. Stoicheff, *ibid.* **71**, 3099 (1993).

[2] J. E. Field, K. H. Hahn, and S. E. Harris, Phys. Rev. Lett. **67**, 3962 (1991); S. E. Harris, J. E. Field, and A. Kasapi, Phys. Rev. A **46**, R29 (1992); K. Hakuta, L. Marmet, and B. P. Stoicheff, Phys. Rev. Lett. **66**, 596 (1991).

[3] M. O. Scully, Phys. Rev. Lett. **67**, 1885 (1991).

[4] A. Kasapi, M. Jain, G. Y. Yin, and S. E. Harris, Phys. Rev. Lett. **74**, 2447 (1995); M. Jain, A. J. Merriam, A. Kasapi, G. Y. Yin, and S. E. Harris, *ibid.* **75**, 4385 (1995).

[5] O. Kocharovskaya and P. Mandel, Phys. Rev. A **42**, 532 (1990).

[6] M. Jain, H. Xia, G. Y. Yin, A. J. Merriam, and S. E. Harris, Phys. Rev. Lett. **77**, 4326 (1996).

[7] J. H. Eberly, R. Rahman, and R. Grobe, Phys. Rev. Lett. **76**, 3687 (1996); R. Grobe, F. T. Hioe, and J. H. Eberly, *ibid.* **73**, 3183 (1996); J. Oreg, F. T. Hioe, and J. H. Eberly, Phys. Rev. A **29**, 690 (1984); A. H. Toor and M. S. Zubairy, *ibid.* **45**, 5297 (1992); C. E. Carroll and F. T. Hioe, *ibid.* **42**, 1522 (1990), and references therein; J. Lawall, Ph.D. dissertation, Harvard University, 1991.

[8] R. K. Wunderlich, W. R. Garrett, R. C. Hart, M. A. Moore, and M. G. Payne, Phys. Rev. A **41**, 6345 (1990).

[9] W. R. Garrett, M. A. Moore, R. C. Hart, M. G. Payne, and R. K. Wunderlich, Phys. Rev. A **45**, 6687 (1992).